Int J Adv Manuf Technol (2017) 93:3395–3408
DOI 10.1007/s00170-017-0718-y

ORIGINAL ARTICLE

# An accurate characterization method to tracing the geometric defect of the machined surface for complex five-axis machine tools

**Dongju Chen**[1,2] · **Hao Wang**[1] · **Ri Pan**[1] · **Jinwei Fan**[1] · **Qiang Cheng**[1]

Received: 23 March 2017 / Accepted: 26 June 2017 / Published online: 17 July 2017


**Abstract** Geometric error is the main error that affects the machining accuracy of complex five-axis machine tool. Therefore, tracing analysis of error influence for a complex machine tool has been carried out based on an S-shaped workpiece in this study. A method of judging the error parameters which is the biggest influence on machining errors is established. In this method, the machining error of S-shaped workpiece and shaping motions of complex machine tool are comprehensively considered. Cubic B-splines surface has been applied to characterization of the curved surface. The actual position of tool center can be deduced by projecting the B-splines surface in its normal direction. The mapping relationship between the actual tool position and the actual machining curve has established. The machining errors generation model has established. The error expression equation has been deduced. Those five key parameters that have great influence on machining errors are determined according to the contribution which have been computed using the sensitivity and measured values of error parameters. Experimental results show that the error of each point is not more than ±1.5 μm by comparing the five error parameters and all parameters under the action of at the same time. The biggest errors which influence on the machining errors are $\varepsilon_{yC_1}$, $\delta_z(B)$, $\varepsilon_y(C_1)$, $\varepsilon_x(C_1)$, and $\varepsilon_{x_1C_1}$.

✉ Dongju Chen
djchen@bjut.edu.cn

[1] Beijing Key Laboratory of Advanced Manufacturing Technology, Beijing University of Technology, Beijing 100124, People's Republic of China

[2] College of Mechanical Engineering & Applied Electronics Technology, Beijing University of Technology, Ping Leyuan 100#, Chaoyang district, Beijing 100124, People's Republic of China

**Keywords** Complex machine tool · Error tracing · Machining error · Sensitivity · S-shaped workpiece

## 1 Introduction

Positioning accuracy is the key factor that affects the machining accuracy of ultra-precision machine tool. At present in the accuracy test and acceptance check of machine tools, it is necessary to use the dual-frequency laser interferometer to detect the positioning accuracy of the movement axis of the machine tool and to require processing of the standard samples of machine tool to achieve the specified accuracy requirements.

At present, the S-shaped parts, cone-body parts, and round-diamond-square parts are widely used as the standard samples. And the machining of these samples needs to utilize the multi-axis linkage function of machine tool. Therefore, the machining errors of these samples are also the results of the comprehensive effect of multiple error factors. The machine tool contains a large number of error sources, and the milling mode of turning and milling composite machine tool is only studied in this paper. Each motion axes has six motion errors, for the five-axis (three translational axes and B, C rotation axes) machine tool, so the error model contains a total of 30 motion errors. Moreover, there are three non-perpendicularity errors between the two translational axes, and the same time, there are 2 non-perpendicularity errors between rotation axis $B$ and axis $X_1$,$Z_1$, there are two non-perpendicularity errors between rotation axis $C_1$ and axis $X_1$,$Y_1$; therefore, the error model has a total of 37 error parameters.

It is a very theoretical and practical research topic to find out the main influencing factors of machining errors by detecting the machining samples and reverse tracing in the many error factors. Generally for the error sources that cannot be measured directly, firstly the intermediate quantities associated with the error

components to be identified are measured with test instruments. Then, the main error components that affect machining accuracy are estimated by an accurate and effective mathematical model of error identification. Therefore, the error identification requires that the measured intermediate quantities have the traceability for the causes of the errors. Lin et al. [1] proposed a method of matrix summation to model the geometric error of five-axis CNC machine tools. This method divides the motion equation into six parts, each of which has a physical meaning. Besides this method significantly reduces the computational effort of the model and makes the five-axis error model easy to understand. Kyoung-gee Ahn et al. [2] used the homogeneous coordinate transformation to establish the geometric error model of the multi-spindle machine tool and solved the corresponding space errors. Suh SH et al. [3]presented a comprehensive procedure for the calibration of the rotary table including geometric error model, error compensation method for the CNC controller, error measurement method, and verification of the error model and compensation algorithm with experimental apparatus. The methods developed were verified by various experiments, showing the validity and effectiveness of the presented methods, indicating they can be used for multiaxis machine tools as a means of calibration and precision enhancement of the rotary table. Using the standard test bar-micro displacement sensor-encoder method, Hong et al. [4] successfully traced the source for the individual movement error. Utilizing the white light interferometer, Kim et al. [5] designed three-dimensional measurement system of the ultra-precision. Jung et al. [6] used a contact probe to perform on-line measurements for the errors of each coordinate direction of machine tool. Gao et al. [7] used the photoelectric autocollimator to detect the spindle skew error and measured the axial runout error with the capacitance displacement probe, and detected the straightness error of the guideway with the ruler and the capacitance displacement probe. Grejda et al. [8] tested the radial and axial runout errors of the nanoscale spindles by using the portable leading shaft and the capacitive probe. A few scholars [9–13] used a laser interferometer to measure the geometric error of NC machine tools. The laser beam was concentrated by using a condenser. The error was compensated with software based on the measured results, and this method reduced the cost of ultra-precision machining. Based on the kinematics model of five-axis machine tools, Ibaraki et al. [14] proposed a set of machining tests for a five-axis machine tool to identify its kinematic errors, one of its most fundamental error sources. In each machining pattern, a simple straight side cutting using a straight end mill is performed. The relationship between geometric errors of the finished workpiece and the machine's kinematic errors is formulated based on the kinematic model of a five-axis machine. A simple straight side cutting using a straight end mill was only performed. However in order to detect more comprehensively, the S-shaped workpiece with the machining features of open angle processing area, closed angle processing area, the processing area of open angle and closed angle conversion and the varying angle between the edge of the surface and the base surface is used as the test workpiece in this article. Lee et al. [15] measured a machine with a ball bar, analyzed the measurement results, and obtained the independent geometric error of the position, and established the corresponding confidence interval in 2013. The correctness of the machining results was verified by experimental compensation. Chen et al. [16] measured the rotation axis of machine tool with a two-step identification method and cue instrument. The identification model was established based on the measured results. The most suitable installation parameter was obtained by sensitivity analysis and the correctness of the model was verified on the four-axis machining center. According to the certain machining conditions, the workpiece surface is machined and the surface morphology of the workpiece can be measured directly to trace the errors. Using the method of surface evaluation, the satisfactory traceability results can be obtained quickly. The profiler and the interferometer are the most frequently used instruments for the measurement of a workpiece [17–19].

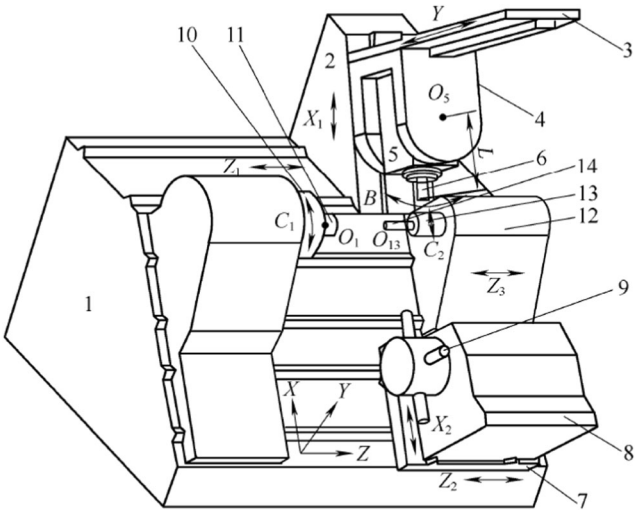


**Fig. 1** The structure map of CHD-25 turning-milling complex machine

**Table 1** The branches of the machine tools

| Number | 1 | 2 | 3 | 4 | 5 | 6 | 7 |
|---|---|---|---|---|---|---|---|
| Name | Bed | Slider in $Z_1$ | Slider in $X_1$ | Slider in $Y$ | Axis $B$ | Tool | Slider in $Z_2$ |
| Number | 8 | 9 | 10 | 11 | 12 | 13 | 14 |
| Name | Slider in $X_2$ | Tool | Axis $C_1$ | Workpiece | Slider in $Z_3$ | Axis $C_2$ | Workpiece |
| Branch 'machine-workpiece' | 1, 10, 11 | | | | | | |
| Branch 'machine-tool' | 1, 2, 3, 4, 5 and 6 | | | | | | |

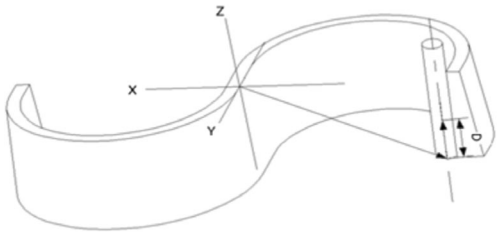


**Fig. 2** Position relationship between cutter and workpiece

According to the mathematical model of the S-shaped workpiece in this study, cubic B-splines surface has been applied to surface representation. The actual position of tool center can be deduced by projecting the B-splines surface in its normal direction. The mapping relationship between the machine tool and the actual machining curve is established. Based on the error analysis theory of multi-body system and the mathematical model of the curved surface, the error expression equation corresponding to each processing point on the surface has been established by utilizing a method of superposition of the tool center position and tool direction vector from the perspective of the machine tool. Besides based on the actual machining of the S-shaped sample of complex CNC machine tool, the model of error parameter sensitivity influencing accuracy of curved surface and the model of impact analysis are established, and a method of reverse tracing analysis for key error parameters is proposed. The influence proportion of each error parameter on the machining accuracy can be obtained, so the identification of key error parameters can be realized and the error parameters which have great influence on machining errors can be found.

## 2 Characterization and analysis of machining errors of complex CNC machine tool

### 2.1 Mathematical model of B-spline surfaces

Because of geometric invariance, continuity, and symmetry, the B-spline surface is widely applied in the field of mechanical processing. For a given number of $(n+1)\times(m+1)$ points, these points $P_{i,j}(i=0,1,\ldots,n; j=0,1,\ldots,m)$ constitute a control grid. Here, the powers of the parameters $u$ and $v$ are $p$ and $q$, respectively. And two node vectors are given as $\mathbf{U}=(u_0, u_1, \cdots, u_{n+p+1})$ and $\mathbf{V}=(v_0, v_1, \cdots, v_{m+p+1})$ respectively. So a B-spline surface with the $p\times q$ power of tensor product can be defined as follows:

$$s(u,w)=\sum_{i=0}^{n}\sum_{j=0}^{m} N_{i,p}(u)N_{j,p}(w)V_{i,j} \tag{1}$$

In the above equation, $N_{i,p}(u)$ is the B-spline basis function with $p$ power of $u$, and $N_{j,q}(w)$ is the B-spline basis function with $q$ powers of $w$, and $V_{i,j}$ are control points of the B-spline surface.

In practical application, generally when the values of $p$ and $q$ are both 3, it can meet the requirement of continuous order of the surface in engineering design; And substituting the values of $p$ and $q$ being both 3 into the above equation, the uniform double cubic B-spline surface is expressed as follows:

$$s(u,w)=\mathbf{U}M_BVM_B^TW_T \quad 0\le u \quad w\le 1 \tag{2}$$

In which

$$\mathbf{U}=\begin{pmatrix}1 & u & u^2 & u^3\end{pmatrix},\quad W=\begin{pmatrix}1 & w & w^2 & w^3\end{pmatrix}$$

$$\mathbf{M}_B=\frac{1}{6}\begin{pmatrix}1 & 4 & 1 & 0\\ -3 & 0 & 3 & 0\\ 3 & -6 & 3 & 0\\ -1 & 3 & -3 & 1\end{pmatrix},\mathbf{V}=\begin{pmatrix}\mathbf{V}_{i-1,j-1} & \mathbf{V}_{i-1,j} & \mathbf{V}_{i-1,j+1} & \mathbf{V}_{i-1,j+2}\\ \mathbf{V}_{i,j-1} & \mathbf{V}_{i,j} & \mathbf{V}_{i,j+1} & \mathbf{V}_{i,j+2}\\ \mathbf{V}_{i+1,j-1} & \mathbf{V}_{i+1,j} & \mathbf{V}_{i+1,j+1} & \mathbf{V}_{i+1,j+2}\\ \mathbf{V}_{i+2,j-1} & \mathbf{V}_{i+2,j} & \mathbf{V}_{i+2,j+1} & \mathbf{V}_{i+2,j+2}\end{pmatrix}$$

The elements in the $V$ matrix in Eq. 2 are the control vertices of the polygon. And the matrix $M_B$ is a coefficient matrix.

### 2.2 Characterization of machining errors of workpiece

The machining process of the workpiece is the process of relative movement between the tool and workpiece—this is called forming movement. The tooling point is the forming point. And the forming path in the workpiece coordinate system is the machined surface of the workpiece. Any machine tool can be decomposed into two branches: the 'machine tool-

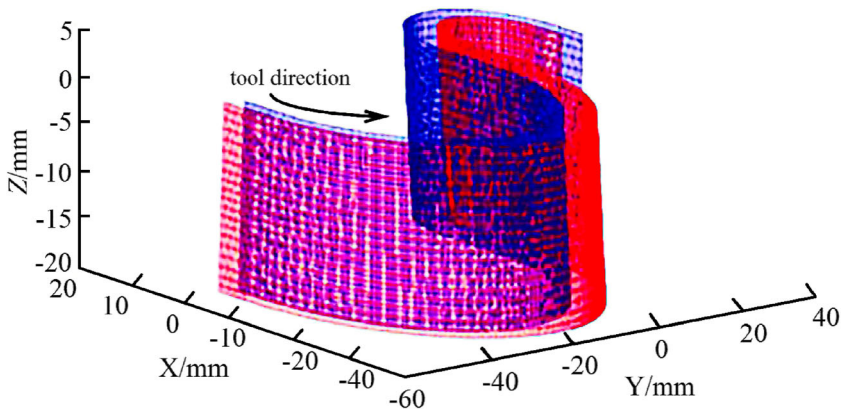


**Fig. 3** The contrast of ideal carved surface and tool center carved surface

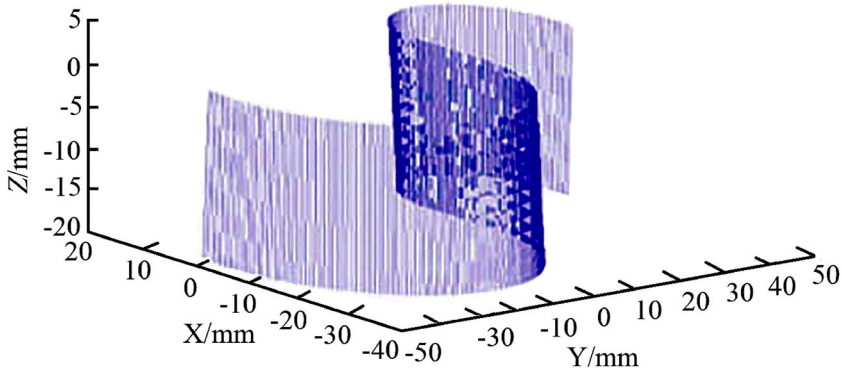


**Fig. 4** The vector diagram of tool direction

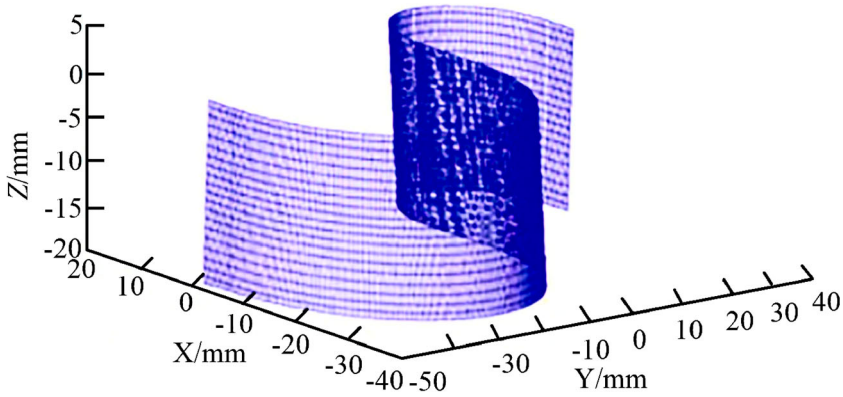


**Fig. 5** The fitting diagram of tool path

tool' branch and 'machine tool-workpiece' branch. Through establishing coordinate systems in various movement bodies and using homogeneous coordinate transformation, the center position and direction vector of the tool described in the tool coordinate system can be transformed into workpiece coordinate and described by transformation matrix of error motion. Therefore, the actual path and actual direction of the tool are obtained.

$$[\mathbf{p}_T]_W = [\mathbf{B}_W]^{-1}[\mathbf{B}_T][\mathbf{p}_T]_T \tag{3}$$

$$[\mathbf{v}_T]_W = [\mathbf{B}_W]^{-1}[\mathbf{B}_T][\mathbf{v}_T]_T \tag{4}$$

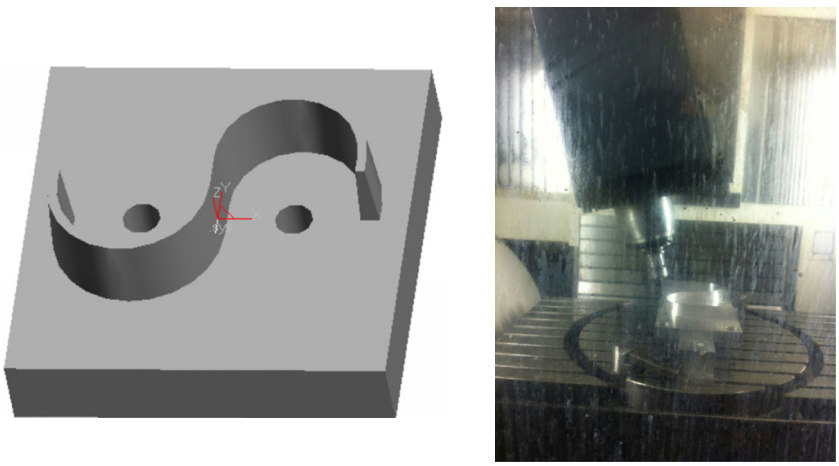

(a)Designed (b) Machined

**Fig. 6** The scene of S-shaped workpiece

**Table 2** Parameters of the CMM

| Measuring accuracy (μm) | Measuring range (mm) | Workpiece weight (Kg) | Resolution (mm) | Position accuracy (mm) | Acceleration (mm/s$^2$) |
|---|---|---|---|---|---|
| (2.1 + $L$)/250 | $X_1$ 700<br>$Y$ 700<br>$Z_1$ 60<br>$B$ −180°~180°<br>$C_1$ 0~360° | 560 | 0.0002 | 0.001 | 1700 |

Where the $[\mathbf{p}_T]_W$ and $[\mathbf{p}_T]_T$ denote the position coordinates of the cutter head in workpiece coordinate system and tool coordinate system respectively. The $[\mathbf{v}_T]_W$and $[\mathbf{v}_T]_T$ denote the projection of the direction vector of the tool in workpiece coordinate system and tool coordinate system respectively. The $[\mathbf{B}_W]$ is the transform matrix of the actual motion of the machine tool-workpiece branch and the $[\mathbf{B}_T]$ is the transform matrix of the actual motion of the machine tool-tool branch.

In this study, the complex CNC machine tool relates to five-axis linkage in the machining process. And the five axis turning-milling multi-functional machine tools contains $X_1$ axis, $Y$ axis, $Z_1$ axis, $B$ axis and $C_1$ axis, the structure is illustrated in Fig. 1. The machine tool-workpiece branch includes 1, 10, and 11. And the machine tool-tool branch includes 1, 2, 3, 4, 5, and 6. Their description is presented in Table 1.

Thus, the transform matrices of the actual motion of the machine tool-workpiece branch and machine tool-tool branch are obtained, respectively, as illustrated below:

$$[\mathbf{B}_W] = [\mathbf{S}_1\ \ 10]_p[\mathbf{S}_1\ \ 10]_{pe}[\mathbf{S}_1\ \ 10]_s[\mathbf{S}_1\ \ 10]_{se}[\mathbf{S}_{10}\ \ 11]_p[\mathbf{S}_{10}\ \ 11]_{pe} \tag{5}$$

$$\begin{aligned}[\mathbf{B}_T] = {} & [\mathbf{S}_{12}]_p[\mathbf{S}_{12}]_{pe}[\mathbf{S}_{12}]_s[\mathbf{S}_{12}]_{se}[\mathbf{S}_{23}]_p[\mathbf{S}_{23}]_{pe}[\mathbf{S}_{23}]_s[\mathbf{S}_{23}]_{se} \\ & [\mathbf{S}_{34}]_p[\mathbf{S}_{34}]_{pe}[\mathbf{S}_{34}]_s\ [\mathbf{S}_{34}]_{se}[\mathbf{S}_{45}]_p[\mathbf{S}_{45}]_{pe}[\mathbf{S}_{45}]_s[\mathbf{S}_{45}]_{se} \\ & [\mathbf{S}_{56}]_p\ [\mathbf{S}_{56}]_{pe}[\mathbf{S}_{56}]_s[\mathbf{S}_{56}]_{se}\end{aligned} \tag{6}$$

The subscript $p$ denotes the relative position of two adjacent objects. The subscript $pe$ denotes the relative position error of two adjacent objects. The subscript $s$ denotes the relative motion of two adjacent objects. And the subscript $se$ denotes the relative motion error of two adjacent objects. The $[\mathbf{S}_{ij}]$ denotes motion transformation matrix.

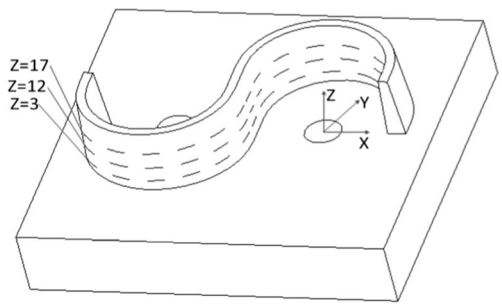


**Fig. 7** The sketch of detecting piece

The following formulas can be obtained by considering Eqs. (3) to (6).

$$[\mathbf{p}_T]_W = [\mathbf{O}_W]^{-1}[\mathbf{O}_T][\mathbf{p}_T]_T \tag{7}$$

$$[\mathbf{v}_T]_W = [\mathbf{O}_W]^{-1}[\mathbf{O}_T][\mathbf{v}_T]_T \tag{8}$$

The $[\mathbf{O}_W]$ denotes the actual motion transformation matrix of machine tool-workpiece branch. The $[\mathbf{O}_T]$ denotes the actual motion transformation matrix of machine tool-tool branch.

### 2.3 Machining error of each point in the S-shaped workpiece

The expressions for the actual tool path and actual tool direction in the workpiece coordinate system are obtained from the above analysis. Based on the error model of the machine tool, the expressions can be used to deduce the equation of machining error for each point on the S-shaped workpiece. Figure 2 illustrates the relationship of relative position between the tool and workpiece in the workpiece coordinate system. The actual position of the tool center whose value distancing from the end face of is $D$ can be expressed as:

$$[\mathbf{p}_a]_W = [\mathbf{p}_T]_W + D \times [\mathbf{v}_T]_W \tag{9}$$

The values of $x_{1a}$, $y_{1a}$ and $z_{1a}$ can be obtained by considering Eqs. (7) to (9). When all the error parameters of $x_{1a}$, $y_{1a}$ and $z_{1a}$ are zero, the position coordinates in an

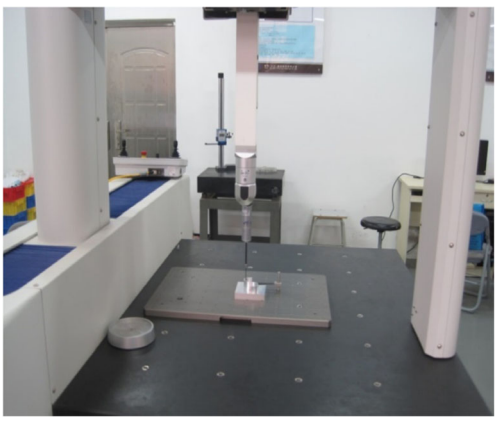

**Fig. 8** The detecting scene of coordinate measuring machine

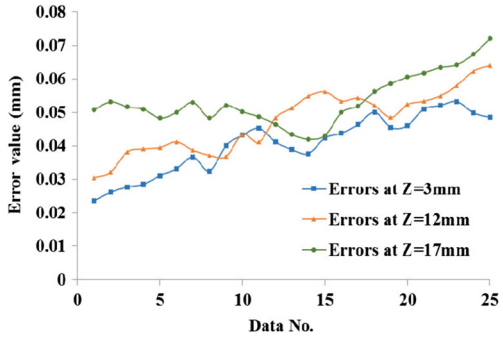


**Fig. 9** Measuring errors of different points

ideal condition can be obtained, and the values are $x_{1I}$, $y_{1I}$ and $z_{1I}$. The $E_x$, $E_y$ and $E_z$ representing the errors in each direction can be obtained by subtracting the ideal values from the actual values.

$$E_x = x_{1a} - x_{1I} \tag{10}$$

$$E_y = y_{1a} - y_{1I} \tag{11}$$

$$E_z = z_{1a} - z_{1I} \tag{12}$$

The coordinates of the location point at the actual conditions are $x_{1a}$, $y_a$ and $z_{1a}$. The coordinates of the location point at the ideal conditions are $x_{1I}$, $y_I$ and $z_{1I}$. $E_x$ denotes the error in the $x$ direction. $E_y$ denotes the error in the $y$ direction. $E_z$ denotes the error in the $z$ direction.

## 3 Reverse tracing analysis of surface errors of S-shaped workpiece

### 3.1 Relationship between tool center point and corresponding machining point of curved surface

Because machining errors of the surface are generated by errors superposition of the machine tool, the corresponding center position of the tool can be obtained by back calculation based on the actual machining point on the surface, and so as to further study the errors of the machine tool. For the curved surface expressed in Eq. (1), the unit normal vector of any point $P(u,v)$ on it can be expressed as:

$$n = \frac{s_u \times s_w}{|s_u \times s_w|} \tag{13}$$

Where $\mathbf{s}_u = (0, 1, 2u, 3u^2)\mathbf{BVB}^T(1, w, w^2, w^3)^T$

$$\mathbf{s}_w = \left(1, u, u^2, u^3\right)\mathbf{BVB}^T\left(0, 1, 2w, 3w^2\right)^T$$

The matrix $\boldsymbol{B}$ is the actual motion transformation matrix.

According to the vector product equation, the following formula can be obtained.

$$\mathbf{s}_u \times \mathbf{s}_w = \begin{vmatrix} \mathbf{i} & \mathbf{j} & \mathbf{k} \\ x_u & y_u & z_u \\ x_w & y_w & z_w \end{vmatrix} = (y_u z_w - y_w z_u)\mathbf{i} - (x_u z_w - x_w z_u)\mathbf{j} + (x_u y_w - x_w y_u)\mathbf{k} \tag{14}$$

When $a = (y_u z_w - y_w z_u), b = (x_u z_w - x_w z_u), c = (x_u y_w - x_w y_u)$;

And the following formula also can be obtained.

$$\mathbf{s}_u \times \mathbf{s}_w = a\mathbf{i} + b\mathbf{j} + c\mathbf{k} \tag{15}$$

$$|\mathbf{s}_u \times \mathbf{s}_w| = \sqrt{a^2 + b^2 + c^2} \tag{16}$$

Substituting the formulas (15) and (16) in Eq. (13), the projections of the unit normal vector in the three coordinate directions are as follows:

$$\begin{cases} x_n = a/\sqrt{a^2 + b^2 + c^2} \\ y_n = b/\sqrt{a^2 + b^2 + c^2} \\ z_n = c/\sqrt{a^2 + b^2 + c^2} \end{cases} \tag{17}$$

The projection of spline surface in the $Z$ direction according to the above methods could be positive or negative. If the $Z$ axis direction of workpiece coordinate is consistent with the $Z$ axis direction of machine tool coordinate, it is defined as the positive direction of the curved surface, and the tool center of the machining curved surface should be biased towards the positive direction of the curved surface. Assuming that the vector $(x_{ps}, y_{ps}, z_{ps})^T$ is component of position vector of a point

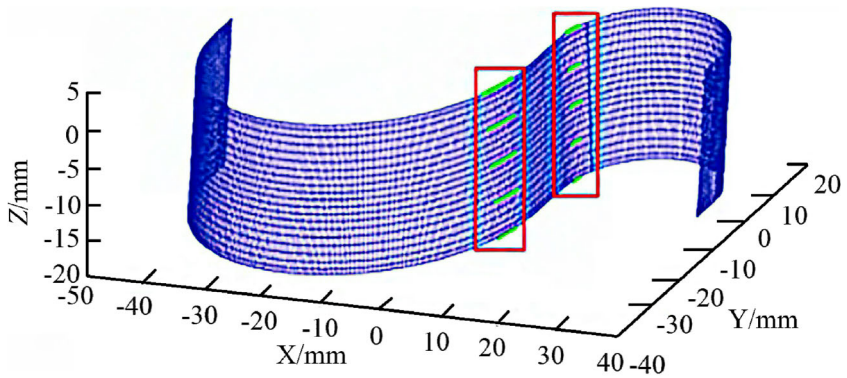


**Fig. 10** The actual machining carved surface

**Table 3** Structure parameters

| Parameter | $q_{wx}$ | $q_{wy}$ | $q_{wz}$ | $q_{5x}$ | $q_{5y}$ | $q_{5z}$ | $L$ |
|---|---|---|---|---|---|---|---|
| Value (mm) | 100 | 100 | 200 | −200 | −200 | −100 | 100 |

on the curved surface in the $X$, $Y$ and $Z$ coordinate direction, respectively, the projector array is expressed as $(x_n, y_n, z_n)^T$ in the normal direction at this point. And the corresponding center position coordinate of the tool is expressed as:

$$\begin{pmatrix} x_p \\ y_p \\ z_p \end{pmatrix} = \begin{pmatrix} x_{ps} \\ y_{ps} \\ z_{ps} \end{pmatrix} + r \begin{pmatrix} x_n \\ y_n \\ z_n \end{pmatrix} \tag{18}$$

where $(x_p, y_p, z_p)^{\mathrm{T}}$is the position array of the tool center, and $r$ is the radius of the tool.

According to the above analysis, as illustrated in Fig. 3, the blue mesh denotes the ideal curved surface and red mesh is the fitting figure of the surface corresponding to tool center surface.

### 3.2 Acquisition of the tool path

During analysis of error effect, it is necessary to use the tool path data to generate the actual tool path. However, acquisition of tool path by using manual programming is more complex. Here, CAXA Manufacturing Engineer software was used to plan the tool path, the data of generated tool path and tool direction vector are simulated by MATLAB software. Figure 4 illustrates the superposed plots for the position and direction of each tool point. The profile showed in the figure based on the obtained data is the S-shape. This verifies the correctness of the extracted data. After the correct tool path and vector data of the tool direction are obtained, the fit figure of curved surface of tool path also can be obtained by the above proposed B-spline surface fitting method, which is illustrated in Fig. 5.

### 3.3 Machining and precision test of S-shaped workpiece

The accuracy of form, position and dimensional precision of machined workpiece reflect machining accuracy of CNC machine tools and they are the combined effects of the errors of all moving parts of the machine tool. And the detecting piece refers to such part which has non-smooth machining surfaces, poor surface quality, poor geometrical accuracy and even occurrence of over cutting in certain special locations. Therefore using the accuracy of machined workpiece is the most direct and effective way to evaluate the geometric errors of the machine. So the S-shaped surface was designed as illustrated in Fig. 6a in this paper. The external dimensions of workpiece is 400 mm × 200 mm and the profile dimensions of the S-shaped is 250 mm × 180 mm. The material of workpiece is the aluminum alloy 7075; And the curved part of the workpiece could be composed of two symmetrical semi-circular B-splines surfaces. As illustrated in the figure, two holes with a diameter 15 mm are utilized to locate for the machining and accuracy test of S-shaped workpiece. The machining site is as illustrated in Fig. 6b. In the actual process, the CAXA Manufacturing Engineer is adopted to accomplish the modeling, the planning of the tool path and verification of correctness based on simulation. Besides the rotation speed of the spindle is 3000 rpm, and the feed velocity along the $X$, $Y$ and $Z$ axes are 24, 16 and 30 m/min, respectively. Finally, the NC machining codes are input into the machine tool for processing by using a post-processing program.

**Table 4** The value of position-independent parameters

| Parameter | $\varepsilon_{x_1z_1}$ | $\varepsilon_{x_1y}$ | $\varepsilon_{x_1C_1}$ | $\varepsilon_{yz_1}$ | $\varepsilon_{x_1B}$ | $\varepsilon_{Bz_1}$ | $\varepsilon_{yC_1}$ |
|---|---|---|---|---|---|---|---|
| Value × $10^{-5}$ (rad) | 2.6 | −0.5 | 2.7 | 1.0 | 1.5 | 3.0 | 4.4 |

The profile measurement of the S-shaped workpiece is mainly carried out by the CMM (Coordinate Measuring Machine) named CMMCMM CONTURA G2, which is produced by the German company Zeiss. And the parameters are presented in Table 2. The contour errors of the S-shaped workpiece were measured at different heights respectively before and after compensation, as illustrated in Fig. 7. The three groups of errors were measured in total, and each group consists of 25 random points. Figure 8 is the measurement site.

When the values of $z$ are 3, 12 and 17 at three different heights, respectively, there are 75 points that are randomly selected. The center of the hole is selected as the origin of reference coordinate system to measure errors in the $X$, $Y$ and $Z$ directions. And the space errors corresponding to each point are calculated. The result of the measurement is illustrated in Fig. 9.

### 3.4 Simulation analysis of the actual tool path and direction

According to the above analysis, it is obvious that the actual tool path must be deviated from the ideal position due to the existence of the errors. And the actual tool path and tool direction can be predicted by considering the generated model of machining errors. The machining errors of the workpiece can be predicted and compensated from the perspective of the machine tool. The actual processing of the S-shaped workpiece described in Section 3.3 is considered as research object. Figure 10 is the curved surface of actual errors which is built by the actual tool path and actual tool direction based on the calculation of formula (1) and formula (2). In the figure, the red wireframe denotes the largest area of space error and the green part denotes the points of maximum error which is calculated. In order to facilitate the analysis, the values of structure parameters are presented in Table 3. Table 4 shows the seven error parameters that have no relationship with the position of the point. In Table 3, the parameter $L$ is the distance from the

**Table 5** The error sensitivity of $x$ axis

| Partial derivative | Expression | Partial derivative | Expression | Partial derivative | Expression |
|---|---|---|---|---|---|
| $\frac{\partial E_x}{\partial \delta_x(x_1)}$ | $\cos C_1$ | $\frac{\partial E_x}{\partial \varepsilon_x(x_1)}$ | $-q_{5z}\sin C_1 - L\sin B\sin C_1 - D\sin B\sin C_1$ | $\frac{\partial E_x}{\partial \delta_y(z_1)}$ | $\sin C_1$ |
| $\frac{\partial E_x}{\partial \delta_x(y)}$ | $\cos C_1$ | $\frac{\partial E_x}{\partial \varepsilon_x(y)}$ | $-q_{5z}\sin C_1 - L\sin B\sin C_1 - D\sin B\sin C_1$ | $\frac{\partial E_x}{\partial \delta_y(B)}$ | $\sin C_1$ |
| $\frac{\partial E_x}{\partial \delta_x(z_1)}$ | $\cos C_1$ | $\frac{\partial E_x}{\partial \varepsilon_x(z_1)}$ | $-q_{5z}\sin C_1 - L\sin B\sin C_1 - D\sin B\sin C_1$ | $\frac{\partial E_x}{\partial \varepsilon_y(x_1)}$ | $q_{5z}\cos C_1 + L\sin B\cos C_1 + D\sin B\cos C_1$ |
| $\frac{\partial E_x}{\partial \delta_x(B)}$ | $\sin B\cos C_1$ | $\frac{\partial E_x}{\partial \delta_y(x_1)}$ | $\sin C_1$ | $\frac{\partial E_x}{\partial \varepsilon_y(y)}$ | $q_{5z}\cos C_1 + L\sin B\cos C_1 + D\sin B\cos C_1$ |
| $\frac{\partial E_x}{\partial \delta_x(C_1)}$ | $-1$ | $\frac{\partial E_x}{\partial \delta_y(y)}$ | $\sin C_1$ | $\frac{\partial E_x}{\partial \varepsilon_y(z_1)}$ | $q_{5z}\cos C_1 + L\sin B\cos C_1 + D\sin B\cos C_1$ |
| $\frac{\partial E_x}{\partial \varepsilon_y(B)}$ | $L\sin B\cos C_1 + D\sin B\cos C_1$ | $\frac{\partial E_x}{\partial \varepsilon_z(z_1)}$ | $q_{5x}\sin C_1 - L\cos B\sin C_1 - q_{5y}\cos C_1 - D\cos B\sin C_1 + x_1\sin C_1 - y\cos C_1$ | $\frac{\partial E_x}{\partial \varepsilon_{Bz_1}}$ | $-L\sin B\sin C_1 - D\sin B\sin C$ |
| $\frac{\partial E_x}{\partial \varepsilon_y(C_1)}$ | $-q_{5z} - L\sin B - z_1 - D\sin B$ | $\frac{\partial E_x}{\partial \varepsilon_z(B)}$ | $-L\sin C_1 - D\sin C_1$ | $\frac{\partial E_x}{\partial \varepsilon_{yC_1}}$ | $L\sin B\cos C_1 + q_{5z}\sin C_1 + z_1\sin C_1 + D\sin B\sin C_1$ |
| $\frac{\partial E_x}{\partial \delta_z(B)}$ | $\sin B\cos C^1$ | $\frac{\partial E_x}{\partial \varepsilon_z(C_1)}$ | $-q_{5x}\sin C_1 + L\cos B\sin C_1 + q_{5y}\cos C_1 + D\cos B\sin C_1 - x_1\sin C_1 + y\cos C_1$ | $\frac{\partial E_x}{\partial \varepsilon_{x_1C_1}}$ | $-q_{5z}\cos C_1 - L\sin B\cos C_1 - z_1\cos C_1 - D\sin B\cos C_1$ |
| $\frac{\partial E_x}{\partial \varepsilon_z(x_1)}$ | $q_{5x}\sin C_1 - L\cos B\sin C_1 - q_{5y}\cos C_1 - D\cos B\sin C_1$ | $\frac{\partial E_x}{\partial \varepsilon_{x_1z_1}}$ | $q_{5z}\cos C_1 + L\sin B\cos C_1 + D\sin B\cos C_1$ | $\frac{\partial E_x}{\partial \varepsilon_{yz_1}}$ | $-q_{5z}\sin C_1 - L\sin B\sin C_1 - z_1\cos C_1 - D\sin B\sin C_1$ |
| $\frac{\partial E_x}{\partial \varepsilon_z(y)}$ | $q_{5x}\sin C_1 - L\cos B\sin C_1 - q_{5y}\cos C_1 - D\cos B\sin C_1$ | $\frac{\partial E_x}{\partial \varepsilon_{x_1y}}$ | $q_{5x}\sin C_1 - L\cos B\sin C_1 - q_{5y}\cos C_1 - D\cos B\sin C_1 - y\cos C_1$ | $\frac{\partial E_x}{\partial \varepsilon_{x_1B}}$ | $-L\cos B\sin C_1 - D\cos B\sin C$ |

center of rotation to the cutter head. The parameters $q_{5x}$, $q_{5y}$ and $q_{5z}$ denote the position coordinates of the intersection $O_5$ between the rotation center axis of the $B$ axis and the center axis of the tool under initial conditions in the machine coordinate system. And the parameters $q_{wx}$, $q_{wy}$ and $q_{wz}$ denote the position coordinates of workpiece coordinate system relative to reference coordinate system of machine tool. In Table 4, these parameters $\varepsilon_{x_1z_1}$, $\varepsilon_{x_1y}$, $\varepsilon_{x_1C_1}$, $\varepsilon_{yz_1}$, $\varepsilon_{x_1B}$, $\varepsilon_{Bz_1}$ and $\varepsilon_{yC_1}$ denote the verticality error between the two axes respectively.

## 4 Analysis of error sensitivity of machine tool

According to the above formulas of the actual position point and tool direction, the accuracy of S-shaped workpiece machined by complex CNC machine tool can be expressed as a function of the 37 error parameters.

$$E = f\left(\delta_i(j), \varepsilon_i(j), \varepsilon_{x_1y}, \varepsilon_{yz_1}, \varepsilon_{x_1z_1}, \varepsilon_{x_1B}, \varepsilon_{Bz_1}, \varepsilon_{x_1C_1}, \varepsilon_{yC_1}\right) \quad (19)$$

where $i = x, y, z; j = x_1, y, z_1, B, C_1$;

The parameter $\varepsilon_i(j)(i = x, y, z; j = x_1, y, z_1, B, C_1)$ denotes the motion angle error around the $x$, $y$ and $z$ axis respectively when moving along each motion axis. The parameter $\delta_i(j)(i = x, y, z; j = x_1, y, z_1, B, C_1)$ denotes the motion displacement error around the $x$, $y$ and $z$ axis respectively when moving along each motion axis. These parameters $x_1$, $y$, $z_1$, $B$ and $C_1$ denote 5 axes of complex five-axis machine tools.

In order to obtain the mathematical expressions of the sensitivity of error parameters, based on Eqs. (10), (11) and (12) respectively, the partial derivatives of the 37 error parameters can be obtained. And they are presented in Tables 5, 6 and 7. From Tables 5, 6 and 7, it is obvious that the error sensitivity of machine tool have relationships with the structure, numerical control instructions and length of cutting tool. The effects on the machine tool are different when the error parameters are different; the machining accuracy of each machined area is also different. The formulas of the error model are in the appendix.

From Eqs. (10), (11) and (12), although the sensitivities of a few error parameters are significantly high, the values of corresponding error parameters are significantly small, and these error parameters have little influence on the point in this case. Therefore, the sensitivity parameters are proposed in this study to evaluate the degree of influence of error parameters and its formula is as follows:

$$\Delta = \frac{\partial E}{\partial u} u \quad (20)$$

Where $u$ is the error parameter, and $E$ is the error.

**Table 6** The error sensitivity of $y$ axis

| Partial derivative | Expression | Partial derivative | Expression | Partial derivative | Expression |
|---|---|---|---|---|---|
| $\frac{\partial E_y}{\partial \delta_x(x_1)}$ | $-\sin C_1$ | $\frac{\partial E_y}{\partial \delta_x(y)}$ | $-\sin C_1$ | $\frac{\partial E_y}{\partial \delta_x(z_1)}$ | $-\sin C_1$ |
| $\frac{\partial E_y}{\partial \delta_x(B)}$ | $-\sin B \sin C_1$ | $\frac{\partial E_y}{\partial \delta_x(C_1)}$ | $-1$ | $\frac{\partial E_y}{\partial \varepsilon_x(B)}$ | $-L\cos C_1\ -D\cos C_1$ |
| $\frac{\partial E_y}{\partial \varepsilon_x(x_1)}$ | $-q_{5z}\cos C_1-\ L\sin B\cos C_1-D\sin B\cos C_1$ | $\frac{\partial E_y}{\partial \varepsilon_x(x_1)}$ | $-q_{5z}\sin C_1-L\sin B\ \sin C_1-D\sin B\sin C_1$ | $\frac{\partial E_y}{\partial \varepsilon_z(C_1)}$ | $-q_{5x}\cos C_1+L\cos B\cos C_1\ -q_{5y}\sin C_1-x_1\cos C_1-y\sin C_1+D\cos B\cos C_1$ |
| $\frac{\partial E_y}{\partial \varepsilon_x(y)}$ | $-q_{5z}\cos C_1-\ L\sin B\cos C_1-D\sin B\cos C_1$ | $\frac{\partial E_y}{\partial \varepsilon_y(y)}$ | $-q_{5z}\sin C_1-L\sin B\ \sin C_1-D\sin B\sin C_1$ | $\frac{\partial E_y}{\partial \varepsilon_{x_1 y}}$ | $q_{5x}\cos C_1-L\cos B\cos C_1\ +q_{5y}\sin C_1+y\sin C_1-D\cos B\cos C_1$ |
| $\frac{\partial E_y}{\partial \varepsilon_x(z_1)}$ | $-q_{5z}\cos C_1-\ L\sin B\cos C_1-D\sin B\cos C_1$ | $\frac{\partial E_y}{\partial \varepsilon_y(z_1)}$ | $-q_{5z}\sin C_1-L\sin B\ \sin C_1-D\sin B\sin C_1$ | $\frac{\partial E_y}{\partial \varepsilon_{x_1 z_1}}$ | $-q_{5z}\sin C_1-L\sin B\sin C_1\ -D\sin B\sin C_1$ |
| $\frac{\partial E_y}{\partial \varepsilon_x(C_1)}$ | $q_{5z}\sin C_1+L\sin B\ +z_1+D\sin B$ | $\frac{\partial E_y}{\partial \varepsilon_y(B)}$ | $-L\sin B\sin C_1-\ D\sin B\sin C_1$ | $\frac{\partial E_y}{\partial \varepsilon_{x_1 C_1}}$ | $q_{5z}\sin C_1+L\sin B\sin C_1\ +z_1\sin C_1+D\sin B\sin C_1$ |
| $\frac{\partial E_y}{\partial \delta_y(x_1)}$ | $\cos C_1$ | $\frac{\partial E_y}{\partial \delta_z(B)}$ | $-\sin B \sin C_1$ | $\frac{\partial E_y}{\partial \varepsilon_{yC_1}}$ | $q_{5z}\cos C_1+L\sin B\cos C_1\ +z_1\cos C_1+D\sin B\cos C_1$ |
| $\frac{\partial E_y}{\partial \delta_y(y)}$ | $\cos C_1$ | $\frac{\partial E_y}{\partial \varepsilon_x(x_1)}$ | $q_{5x}\cos C_1-L\cos B\cos C_1\ +q_{5y}\sin C_1+y\sin C_1-D\cos B\cos C_1$ | $\frac{\partial E_y}{\partial \varepsilon_{yz_1}}$ | $-L\sin B\cos C_1\ -D\sin B\cos C_1$ |
| $\frac{\partial E_y}{\partial \delta_y(z_1)}$ | $\cos C_1$ | $\frac{\partial E_y}{\partial \varepsilon_z(y)}$ | $q_{5z}\sin C_1+q_{5x}\cos C_1\ -L\cos B\cos C_1-D\cos B\cos C_1$ | $\frac{\partial E_y}{\partial \varepsilon_{x_1 B}}$ | $-L\cos B\cos C_1\ -D\cos B\cos C_1$ |
| $\frac{\partial E_y}{\partial \delta_y(B)}$ | $\cos C_1$ | $\frac{\partial E_y}{\partial \varepsilon_x(z_1)}$ | $q_{5x}\cos C_1-L\cos B\cos C_1\ +q_{5y}\sin C_1+y\sin C_1+y\sin C_1-D\cos B\cos C_1$ | $\frac{\partial E_y}{\partial \varepsilon_{Bz_1}}$ | $-L\sin B\cos C_1\ -D\sin B\cos C_1$ |

At present, a method based on the machining accuracy of the workpiece is widely applied to evaluate machining accuracy of the NC machine tool. However, the influence of geometric error, thermal deformation, mechanical vibration and other comprehensive factors on machine tools is different. Thus the machining errors reflected in the test workpiece are also different. It is very important to track reversely the factors that have a greater impact on the basis of the accuracy of the test workpiece. To solve this problem, the main geometric error parameters that affect the machining accuracy are tracked reversely according to the machining errors of S-shaped workpiece in this section. In Fig.2, the points which

**Table 7** The error sensitivity of $z$ axis

| Partial derivative | Expression | Partial derivative | Expression | Partial derivative | Expression |
|---|---|---|---|---|---|
| $\frac{\partial E_z}{\partial \delta_x(B)}$ | $-\sin B$ | $\frac{\partial E_z}{\partial \varepsilon_y(y)}$ | $-q_{5x}+L\cos B+D\cos B$ | $\frac{\partial E_z}{\partial \delta_z(z_1)}$ | 1 |
| $\frac{\partial E_z}{\partial \varepsilon_x(x_1)}$ | $q_{5y}+y$ | $\frac{\partial E_z}{\partial \varepsilon_y(z_1)}$ | $-q_{5x}+L\cos B\ +D\cos B-x_1$ | $\frac{\partial E_z}{\partial \delta_z(B)}$ | $\cos B$ |
| $\frac{\partial E_z}{\partial \varepsilon_x(y)}$ | $q_{5y}$ | $\frac{\partial E_z}{\partial \varepsilon_y(B)}$ | $L\cos B+D\cos B$ | $\frac{\partial E_z}{\partial \delta_z(C_1)}$ | $-1$ |
| $\frac{\partial E_z}{\partial \varepsilon_x(z_1)}$ | $q_{5y}+y$ | $\frac{\partial E_z}{\partial \varepsilon_y(C_1)}$ | $q_{5x}\cos C_1-L\cos B\cos C_1\ +q_{5y}\sin C_1+x_1\cos C_1+y\sin C_1-D\cos B\cos C_1$ | $\frac{\partial E_z}{\partial \varepsilon_{x_1 z_1}}$ | $-q_{5x}+L\cos B\ +D\cos B-x_1$ |
| $\frac{\partial E_z}{\partial \delta_z(x_1)}$ | 1 | $\frac{\partial E_z}{\partial \varepsilon_x(C_1)}$ | $q_{5x}\sin C_1-L\cos B\sin C_1\ +q_{5y}\cos C_1+x_1\sin C_1+y\cos C_1\ -D\cos B\sin C_1$ | $\frac{\partial E_z}{\partial \varepsilon_{yz_1}}$ | $-q_{5y}+y$ |
| $\frac{\partial E_z}{\partial \varepsilon_y(x_1)}$ | $-q_{5x}+L\cos B\ +D\cos B$ | $\frac{\partial E_z}{\partial \delta_z(y)}$ | 1 | $\frac{\partial E_z}{\partial \varepsilon_{x_1 C_1}}$ | $q_{5x}-L\cos B\ -D\cos B+x_1$ |
| $\frac{\partial E_z}{\partial \varepsilon_{yC_1}}$ | $-q_{5y}-y$ | | | | |

**Table 8** The error values and orders of feature points

| No. | $x$ | $y$ | $z$ | Space error | No. | $x$ | $y$ | $z$ | Space error |
|---|---|---|---|---|---|---|---|---|---|
| 1 | 6.75718 | 8.66608 | 0.274 | 0.025326 | 21 | 5.22561 | −13.3305 | −4.7165 | 0.025125 |
| 2 | 6.59275 | 8.01246 | 0.274 | 0.025284 | 22 | 6.05461 | −10.1823 | −4.7165 | 0.025118 |
| 3 | 6.85071 | 8.99054 | 0.274 | 0.025276 | 23 | 5.98878 | −10.5018 | −4.7165 | 0.025113 |
| 4 | 7.05414 | 8.58406 | −4.7165 | 0.025246 | 24 | 4.72372 | −13.8439 | 0.274 | 0.025108 |
| 5 | 5.12671 | −12.6205 | 0.274 | 0.02522 | 25 | 6.11536 | −9.86302 | −4.7165 | 0.025098 |
| 6 | 5.21862 | −12.3113 | 0.274 | 0.025215 | 26 | 7.64805 | 8.42002 | −14.6975 | 0.025096 |
| 7 | 5.03196 | −12.9287 | 0.274 | 0.025213 | 27 | 5.12106 | −13.6403 | −4.7165 | 0.025077 |
| 8 | 5.54598 | −11.0666 | 0.274 | 0.02521 | 28 | 7.06797 | 7.24361 | −9.707 | 0.02507 |
| 9 | 5.47085 | −11.3777 | 0.274 | 0.025207 | 29 | 7.49444 | 7.80961 | −14.6975 | 0.025068 |
| 10 | 4.93315 | −13.2337 | 0.274 | 0.025198 | 30 | 5.90009 | −12.166 | −9.707 | 0.025067 |
| 11 | 6.82561 | 7.62169 | −4.7165 | 0.02519 | 31 | 6.14549 | −11.2088 | −9.707 | 0.025063 |
| 12 | 5.75248 | −10.1221 | 0.274 | 0.025181 | 32 | 5.61948 | −13.1144 | −9.707 | 0.025062 |
| 13 | 6.95315 | 9.31331 | 0.274 | 0.025166 | 33 | 6.29018 | −10.5655 | −9.707 | 0.025058 |
| 14 | 5.81248 | −9.80669 | 0.274 | 0.025159 | 34 | 4.61263 | −14.1484 | 0.274 | 0.025052 |
| 15 | 5.86994 | −9.48977 | 0.274 | 0.025151 | 35 | 5.51808 | −13.4273 | −9.707 | 0.025046 |
| 16 | 7.19387 | 7.87723 | −9.707 | 0.025144 | 36 | 7.73518 | 8.72238 | −14.6975 | 0.025042 |
| 17 | 5.76963 | −11.4528 | −4.7165 | 0.025142 | 37 | 5.01379 | −13.9477 | −4.7165 | 0.025027 |
| 18 | 5.92332 | −9.17246 | 0.274 | 0.025136 | 38 | 7.866 | 8.041 | −19.688 | 0.025021 |
| 19 | 5.32572 | −13.0216 | −4.7165 | 0.025136 | 39 | 7.53808 | 9.11966 | −9.707 | 0.025014 |
| 20 | 5.84574 | −11.1377 | −4.7165 | 0.025132 | 40 | 4.49894 | −14.4494 | 0.274 | 0.025005 |
| 97 | 6.78049 | −9.64819 | −14.6975 | 0.024957 | 100 | 5.19032 | −14.3627 | −9.707 | 0.024893 |
| 98 | 5.30386 | −14.0515 | −9.707 | 0.02495 | 101 | 6.103 | −13.621 | −19.688 | 0.024889 |
| 99 | 4.38111 | −14.7487 | 0.274 | 0.024943 | 102 | 4.2598 | −15.0477 | 0.274 | 0.024888 |

locate in the larger machining error area are sorted according to the size of the errors. Then the 102 points with the maximum error values are selected. Sensitivities of 37 geometric errors at the 102 points are calculated, and the average of the degree of influence of each individual error parameter at the 102 points is provided. Finally the normalization processing is carried out and the geometric error parameters that have high influence on area error are identified. The steps for finding the solution are as follows:

**Table 9** The mean influences of error parameters

| No. | Error parameter | Effect degree | No. | Error parameter | Effect degree |
|---|---|---|---|---|---|
| 1 | $\varepsilon_{yC_1}$ | 0.009666 | 20 | $\varepsilon_y(x_1)$ | 0.001327 |
| 2 | $\delta_z(B)$ | 0.007318 | 21 | $\varepsilon_y(z_1)$ | 0.001304 |
| 3 | $\varepsilon_y(C_1)$ | 0.007236 | 22 | $\varepsilon_{x_1y}$ | 0.001133 |
| 4 | $\varepsilon_x(C_1)$ | 0.005967 | 23 | $\delta_z(x_1)$ | 0.000876 |
| 5 | $\varepsilon_{x_1C_1}$ | 0.005589 | 24 | $\delta_x(z_1)$ | 0.000694 |
| 6 | $\varepsilon_{bz_1}$ | 0.003326 | 25 | $\delta_y(z_1)$ | 0.000673 |
| 7 | $\delta_y(x_1)$ | 0.003102 | 26 | $\varepsilon_x(x_1)$ | 0.000634 |
| 8 | $\delta_y(C_1)$ | 0.002908 | 27 | $\varepsilon_z(C_1)$ | 0.000568 |
| 9 | $\varepsilon_{yz_1}$ | 0.00282 | 28 | $\varepsilon_y(B)$ | 0.000315 |
| 10 | $\delta_y(B)$ | 0.0024 | 29 | $\delta_y(y)$ | 0.000267 |
| 11 | $\varepsilon_z(z_1)$ | 0.002339 | 30 | $\delta_x(y)$ | 0.000185 |
| 12 | $\delta_x(B)$ | 0.002272 | 31 | $\delta_z(y)$ | 0.000182 |
| 13 | $\varepsilon_{x_1z_1}$ | 0.00207 | 32 | $\varepsilon_z(B)$ | 0.000176 |
| 14 | $\delta_z(C_1)$ | 0.001986 | 33 | $\varepsilon_y(y)$ | 0.000127 |
| 15 | $\delta_z(Z_1)$ | 0.001967 | 34 | $\varepsilon_{x_1B}$ | 0.000103 |
| 16 | $\delta_x(C_1)$ | 0.001922 | 35 | $\varepsilon_y(y)$ | 3.39E-05 |
| 17 | $\delta_x(x_1)$ | 0.001863 | 36 | $\varepsilon_x(y)$ | 2.36E-05 |
| 18 | $\delta_x(z_1)$ | 0.001714 | 37 | $\varepsilon_x(B)$ | 3.34E-06 |
| 19 | $\varepsilon_z(x_1)$ | 0.001339 | | | |

(1) Calculation and sorting of comprehensive error of each point.

The error expressions have been provided for the various points in the $x$, $y$ and $z$ directions respectively. Therefore the expression of space error can be obtained, and it is shown below.

$$E_V = \sqrt{E_x^2 + E_y^2 + E_z^2} \tag{21}$$

The $E_x$, $E_y$ and $E_z$ are the errors of a point along the $X$, $Y$and $Z$ directions respectively.

The correlative parameters of each point are substituted into the above formula, and the larger processing error area is determined according to the sizes of the comprehensive errors. Points in the larger processing error area are sorted according to the value of errors. Then the 102 points with the largest errors are selected as description points of the features.

(2) Calculation of average value of influence degree of individual error parameter.

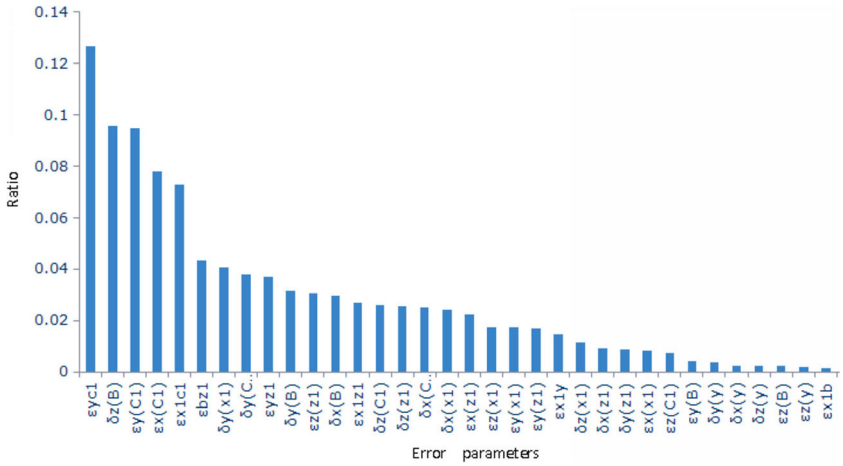


**Fig. 11** The ratio of all the error parameters influence on machining accuracy

According to the above analysis, the correlative parameters of the 102 points are substituted into the expressions of sensitivity. And the influence degree of each point is calculated by Eq. (20). The expression is as follows for influence degree of individual error parameter.

$$\Delta_u = \sqrt{\left(\frac{\partial E_x}{\partial u}u\right)^2 + \left(\frac{\partial E_y}{\partial u}u\right)^2 + \left(\frac{\partial E_z}{\partial u}u\right)^2} \tag{22}$$

Where $u$ is the individual error parameter.

(3) Calculation of average value of influence degree of individual error parameter

For an error parameter, the influence degrees at different points are different. In order to analyze the incremental contribution of the error parameters to the region error, the average value of influence degree of individual error parameter of the 102 points is obtained. Therefore it can reflect the size of the effect of the error, which is calculated as follows:

$$\overline{\Delta}_u = \frac{\Sigma \Delta_{ui}}{102} \quad (i = 1, 2, \ldots, 102) \tag{23}$$

Where $\Delta_{ui}$ is average value of influence degree of individual error parameter at point $i$.

The feature points are 102 points which locate in the larger error area in Section 3.4, and they are sorted according to space error. The results are presented in Table 8, and the results in Table 8 are theoratical. The $x$, $y$ and $z$ are coordinates of the points of the larger error value corresponding to the ideal location points in the workpiece coordinate system. The values of space errors of 102 feature points are obtained by using Eq. (21). The average values of influence degree of individual error parameter are presented in Table 9.

In order to more intuitively analyze the influence of the individual error parameters on the final machining accuracy, the average values of the individual error parameter are normalized in Table 9.

$$V_u = \frac{S_u}{\Sigma S_u} \tag{24}$$

Where the $u$ is the error parameter, and the $S_u$ is the average value of the influence degree corresponding to error parameter.

After the above normalization, the influence proportion of each error parameter on the machining accuracy is obtained, as illustrated in Fig. 11.

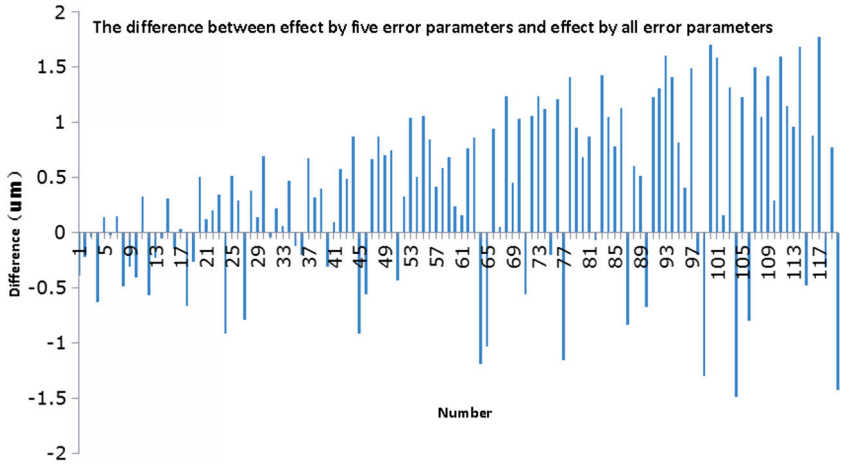


**Fig. 12** The effect difference of five error parameters and all error parameters

After calculation, the error parameters $\varepsilon_{yC_1}$, $\delta_z(B)$, $\varepsilon_y(C_1)$, $\varepsilon_x(C_1)$ and $\varepsilon_{x_1C_1}$ obtained accounted for the total error ratio of 46.8%.Therefore the five error parameters have maximum influence. In order to verify the correctness of the analysis, the results are shown in Fig. 12, and it is the difference between space error of each point of the simultaneous action of the 5 errors and space error of each point of the simultaneous action of the all errors. The maximum difference does not exceed ±1.5 μm. Therefore this demonstrates the correctness of the analysis.

## 5 Conclusion

(1) The method is a study for the error tracing of the complex CNC machine tools based on S-shaped workpiece. Based on the error analysis theory of multi-body system and the mathematical model of the curved surface, the error expression equation corresponding to each processing point on the surface has been established by utilizing a method of superposition of the tool center position and tool direction vector.

(2) Based on the actual machining of the S-shaped sample of complex CNC machine tools, the model of error parameter sensitivity influencing accuracy of curved surface and impact analysis is established and a method of reverse tracing analysis for key error parameters is proposed.

(3) The five key parameters that have great influence on machining errors are determined according to the contribution which have been computed using the sensitivity and measured values of error parameters. The results show that the error of each point is not more than ±1.5 μm by comparing the five error parameters and all parameters under the action of at the same time. The biggest errors which influence on the machining errors are $\varepsilon_{yC_1}$, $\delta_z(B)$, $\varepsilon_y(C_1)$, $\varepsilon_x(C_1)$ and $\varepsilon_{x_1C_1}$. The method is suitable for the machining of complex machine tool, through the diagnosis of these five error parameters, the quality of the workpiece can be improved.

**Acknowledgments** This project is supported by the National Natural Science Foundation of China (Grant 51475010), Beijing Nova program (Z161100004916156), Natural Science Foundation of Beijing Municipality (Grant No. 3142005), and Ultra-precision Machining Technology Key Laboratory Major Fund of China Academy of Engineering Physics (ZZ14002).

**Compliance with ethical standards**

**Conflicts of interest** The authors declare no conflict of interest.

## Appendix

The formulas of the error model in three directions are shown.

$$
\begin{aligned}
E_x = {} & \delta_x(x_1)\cos C_1 + \delta_x(y)\cos C_1 + \delta_x(z_1)\cos C_1 + \delta_x(B)\cos C_1 - \delta_x(C_1) + q_{5z}\varepsilon_{x_1z_1} \\
& \cos C_1 + q_{5z}\varepsilon_y(x_1)\cos C_1 + q_{5z}\varepsilon_y(y)\cos C_1 + q_{5z}\varepsilon_y(z_1)\cos C_1 - q_{5y}\varepsilon_z(y)\cos C_1 + \delta_z(B) \\
& \sin B\cos C_1 + L\varepsilon_{x_1z_1}\sin B\cos C_1 + L\varepsilon_y\sin B\cos C_1 + L\varepsilon_y(x_1)\sin B\cos C_1 + L\varepsilon_y(y) \\
& \sin B\cos C_1 + L\varepsilon_y(z_1)\sin B\cos C_1 - q_{5x}\varepsilon_z(C_1)\sin C_1 + L\varepsilon_z(C_1)\cos B\sin C_1 + q_{5x}\varepsilon_z(z_1) \\
& \sin C_1 - L\varepsilon_z(z_1)\cos B\sin C_1 - q_{5z}\varepsilon_{x_1C_1}\cos C_1 + q_{5z}\varepsilon_{yC_1}\sin C_1 - q_{5z}\varepsilon_y(C_1) - L\varepsilon_{x_1C_1}\sin B \\
& \cos C_1 + L\varepsilon_{yC_1}\sin B\sin C_1 - L\varepsilon_y(C_1)\sin B - L\varepsilon_z(B)\sin C_1 + \delta_y(x_1)\sin C_1 + \delta_y(y)\sin C_1 \\
& + \delta_y(z_1)\sin C_1 + \delta_y(B)\sin C_1 + q_{5x}\varepsilon_{x_1y}\sin C_1 - q_{5z}\varepsilon_{yz_1}\sin C_1 - q_{5z}\varepsilon_x\sin C_1 - q_{5z}\varepsilon_x(y) \\
& \sin C_1 - q_{5z}\varepsilon_x(z_1)\sin C_1 + q_{5x}\varepsilon_z(x_1)\sin C_1 + q_{5x}\varepsilon_z(y)\sin C_1 - L\varepsilon_{x_1B}\cos B\sin C_1 - L\varepsilon_{x_1y} \\
& \cos B\sin C_1 - L\varepsilon_z(x_1)\cos B\sin C_1 - L\varepsilon_z(y)\cos B\sin C_1 - L\varepsilon_{Bz_1}\sin B\sin C_1 - L\varepsilon_{yz_1}\sin B \\
& \sin C_1 - L\varepsilon_x(x_1)\sin B\sin C_1 - L\varepsilon_x(y)\sin B\sin C_1 - L\varepsilon_x(z_1)\sin B\sin C_1 - q_{5y}\varepsilon_{x_1y}\cos C_1 \\
& + q_{5y}\varepsilon_z(C_1) - q_{5y}\varepsilon_z(x_1)\cos C_1 - q_{5y}\varepsilon_z(z_1)\cos C_1 + x_1(-\varepsilon_z(C_1)\sin C_1 + \varepsilon_z(z_1)\sin C_1) \\
& - y\left(\varepsilon_{x_1y}\cos C_1 - \varepsilon_z(C_1)\cos C_1 + \varepsilon_z(x_1)\cos C_1 + \varepsilon_z(z_1)\cos C_1\right) - z_1(\varepsilon_{x_1C_1}\cos C_1 - \varepsilon_{yC_1}\cos C_1 \\
& + \varepsilon_y(C_1)) + D\left(\varepsilon_{x_1z_1}\sin B\cos C_1 + \varepsilon_y(B)\sin B\cos C_1 + \varepsilon_y(x_1)\sin B\cos C_1 + \varepsilon_y(y)\sin B\cos C_1\right) \\
& + \varepsilon_y(z_1)\sin B\cos C_1 + \varepsilon_z(C_1)\cos B\sin C_1 - \varepsilon_z(B)\sin C_1 - \varepsilon_{x_1B}\cos B\sin C_1 - \varepsilon_{x_1y}\cos B\sin C_1 \\
& - \varepsilon_z(x_1)\cos B\sin C_1 - \varepsilon_z(y)\cos B\sin C_1 - \varepsilon_z(z_1)\cos B\sin C_1 - \varepsilon_{Bz_1}\sin B\sin C_1 - \varepsilon_{yz_1}\sin B \\
& \sin C_1 - \varepsilon_x(x_1)\sin B\sin C_1 - \varepsilon_x(y)\sin B\sin C_1 - \varepsilon_x(z_1)\sin B\sin C_1 + \varepsilon_{yC_1}\sin B\sin C_1 - \varepsilon_{x_1C_1} \\
& \sin B\cos C_1 - \varepsilon_y(C_1)\sin B)
\end{aligned}
$$

$$E_y = -\delta_x(x_1)\sin C_1 - \delta_x(y)\sin C_1 - \delta_x(z_1)\sin C_1 - q_{5z}\varepsilon_{x_1z_1}\sin C_1 - q_{5z}\varepsilon_y(x_1)\sin C_1 - q_{5z}\varepsilon_y(y)\sin C_1 - q_{5z}\varepsilon_y(z_1)\sin C_1 + q_{5z}\varepsilon_z(y)\sin C_1 - \delta_x(B)\cos B\sin C_1 - \delta_z(B)\sin B\sin C_1 - \delta_y(C_1) - L\varepsilon_{x_1z_1}\sin B\sin C_1 - L\varepsilon_y\sin B\sin C_1 - L\varepsilon_y(x_1)\sin B\sin C_1 - L\varepsilon_y(y)\sin B\sin C_1 - L\varepsilon_y(z_1)\sin B\cos C_1 - q_{5x}\varepsilon_z(C_1)\cos C_1 + q_{5x}\varepsilon_z(z_1)\cos C_1 + L\varepsilon_z(C_1)\cos B\cos C_1 - L\varepsilon_z(z_1)\cos B\cos C_1 + q_{5z}\varepsilon_{yC_1}\cos C_1 + q_{5z}\varepsilon_{x_1C_1}\sin C_1 + q_{5z}\varepsilon_x(C_1)\sin C_1 + L\varepsilon_{yC_1}\sin B\cos C_1 + L\varepsilon_{x_1C_1}\sin B\sin C_1 + L\varepsilon_x(C_1)\sin B - L\varepsilon_z(B)\cos C_1 + \delta_y(x_1)\cos C_1 + \delta_y(y)\cos C_1 + \delta_y(z_1)\cos C_1 + \delta_y(B)\cos C_1 + q_{5z}\varepsilon_{x_1y}\cos C_1 - q_{5z}\varepsilon_{yz_1}\cos C_1 - q_{5z}\varepsilon_x(x_1)\cos C_1 - q_{5z}\varepsilon_x(y)\cos C_1 - q_{5z}\varepsilon_x(z_1)\cos C_1 + q_{5x}\varepsilon_z(x_1)\cos C_1 + q_{5x}\varepsilon_z(y)\cos C_1 - L\varepsilon_{x_1B}\cos B\cos C_1 - L\varepsilon_{x_1y}\cos B\cos C_1 - L\varepsilon_z(x_1)\cos B\cos C_1 - L\varepsilon_z(y)\cos B\cos C_1 - L\varepsilon_{Bz_1}\sin B\cos C_1 - L\varepsilon_{yz_1}\sin B\cos C_1 - L\varepsilon_x(x_1)\sin B\cos C_1 - L\varepsilon_x(y)\sin B\cos C_1 - L\varepsilon_x(z_1)\sin B\cos C_1 + q_{5x}\varepsilon_{x_1y}\sin C_1 - q_{5y}\varepsilon_z(C_1)\sin C_1 + q_{5y}\varepsilon_z(x_1)\sin C_1 + q_{5y}\varepsilon_z(z_1)\sin C_1 + x_1(\varepsilon_z(z_1)\cos C_1 + \varepsilon_z(C_1)\cos C_1) + y(\varepsilon_{x_1y}\sin C_1 - \varepsilon_z(C_1)\sin C_1 + \varepsilon_z(x_1)\sin C_1 + \varepsilon_z(z_1)\sin C_1) + z_1\left(\varepsilon_{yC_1}\cos C_1 - \varepsilon_{x_1C_1}\sin C_1 + \varepsilon_x(C_1)\right) + D(\varepsilon_{yC_1}\sin B\cos C_1 + \varepsilon_{x_1C_1}\sin B\sin C_1 + \varepsilon_x(C_1)\sin B - \varepsilon_z(B)\cos C_1 - \varepsilon_{x_1B}\cos B\cos C_1 - \varepsilon_{x_1y}\cos B\cos C_1 - \varepsilon_z(x_1)\cos B\cos C_1 - \varepsilon_y(y)\cos B\cos C_1 - \varepsilon_z(z_1)\cos B\cos C_1 - \varepsilon_{Bz1}\sin B\cos C_1 - \varepsilon_{yz_1}\sin B\sin C_1 - \varepsilon_x(x_1)\sin B\sin C_1 - \varepsilon_z(y)\sin B\sin C_1 - \varepsilon_x(z_1)\sin B\cos C_1 + \varepsilon_z(C_1)\cos B\cos C_1 - \varepsilon_{x_1z_1}\sin B\sin C_1 - \varepsilon_y\sin B\sin C_1 - \varepsilon_y(x_1)\sin B\sin C_1 - \varepsilon_y(y)\sin B\sin C_1 - \varepsilon_y(z_1)\sin B\sin C_1)$$

$$E_z = q_{5x}\varepsilon_y(C_1)\cos C_1 + q_{5x}\varepsilon_x(C_1)\sin C_1 + q_{5x}\varepsilon_{x_1C_1} - q_{5x}\varepsilon_{x_1z_1} - q_{5x}\varepsilon_y(z_1) - L\varepsilon_y(C_1)\cos B\cos C_1 - L\varepsilon_x(C_1)\cos B\sin C_1 - L\varepsilon_{x_1C_1}\cos B + L\varepsilon_{x_1z_1}\cos B + L\varepsilon_y(z_1)\cos B + q_{5y}\varepsilon_y(C_1)\sin C_1 - q_{5y}\varepsilon_x(C_1)\cos C_1 - q_{5y}\varepsilon_{yC_1} - q_{5y}\varepsilon_{yz_1} + q_{5y}\varepsilon_x(x_1) + q_{5y}\varepsilon_x(z_1) + \delta_z(x_1) - \delta_z(C_1) + \delta_z(y) + \delta_z(z_1) + \delta_z(B)\cos B + q_{5y}\varepsilon_x(y) - q_{5x}\varepsilon_y(x_1) - q_{5x}\varepsilon_y(y) - \delta_x(B)\sin B + L\varepsilon_y(B)\cos B + L\varepsilon_y(x_1)\cos B + L\varepsilon_y(y)\cos B + x_1\left(\varepsilon_y(C_1)\right)\cos C_1 + \varepsilon_x(C_1)\sin C_1 + \varepsilon_{x_1C_1} - \varepsilon_{x_1z_1} - \varepsilon_y(z_1)) + y\Big(\varepsilon_y(C_1)\sin C_1 - \varepsilon_x(C_1)\cos C_1 - \varepsilon_{yC_1} + \varepsilon_{yz_1} + \varepsilon_x(x_1) + \varepsilon_x(z_1)) + D\Big(-\varepsilon_y(C_1)\cos B\cos C_1 - \varepsilon_x(C_1)\cos B\sin C_1 - \varepsilon_{x_{1C_1}}\cos B + \varepsilon_{x_1z_1}\cos B + \varepsilon_y(B)\cos B + \varepsilon_y(x_1)\cos B + \varepsilon_y(y)\cos B + \varepsilon_y(z_1)\cos B)$$

## References


1. Lin Y, Shen Y (2003) Modeling of five-axis machine tool metrology models using the matrix summation approach. Int J Adv Manuf Technol 21(4):243–248
2. Ahn K-G, Min B-K, Pasek ZJ (2006) Modeling and compensation of geometric rrrors in simultaneous cutting using a multi-spindle machine tool. Int J Adv Manuf Technol 29(9–10):929–939
3. Suh SH, Lee ES, Jung SY (1998) Error modelling and measurement for the rotary table of five-axis machine tools. Int J Adv Manuf Technol 14(9):656–663
4. Hong S, Shin Y, Lee H (1997) An efficient method for identification of motion error sources from circular test results in NC machines. Int J Mach Tools Manuf 37:327–340
5. Kim D-S, Chang I-C, Kim S-W (2002) Microscopic topographical analysis of tool vibration effects on diamond turned optical surfaces. Precision Engineering 26:168–174
6. Jung J-H, Choi J-P, Lee S-J (2006) Machining accuracy enhancement by compensating for volumetric errors of a machine tool and on-machine measurement. J Mater Process Technol 174:56–66
7. Gao W, Tano M, Araki T (2007) Measurement and compensation of error motions of a diamond turning machine. Precis Eng 313:10–316
8. Gao W, Aoki J, Ju BF (2007) Surface profile measurement of a sinusoidal grid using an atomic force microscope on a diamond turning machine. Precis Eng 31:304–309
9. Barman S, Sen R (2010) Enhancement of accuracy of multi-axis machine tools through error measurement and compensation of errors using laser interferometry technique. J Metrol Soc India 25: 79–87
10. Wang JD, Guo JJ (2012) Research on volumetric error compensation for NC machine tool based on laser tracker measurement. Sci China Technol Sci 55:3000–3009
11. Barman S, Sen R (2012) Performance evaluation of multi-axis CNC machine tools by interferometry principle using laser calibration system. J Inst Eng 93:151–155
12. Chen GS, Mei XS, Li HL (2013) Geometric error modeling and compensation for large-scale grinding machine tools with multi-axes. Int J Adv Manuf Technol 69:2583–2592
13. Li DX, Zhang JF, Zhang YL, Feng PF (2014) Modeling, identification and compensation for geometric errors of laser annealing table. J Central South Univ 21:904–911
14. Ibaraki S, Sawada M, Matsubara A (2010) Machining tests to identify kinematic errors on five-axis machine tools. Precis Eng 34:387–398

15. Lee K-I, Yang S-H (2013) Measurement and verification of position-independent geometric errors of a five-axis machine tool using a double ball-bar. Int J Mach Tools Manuf 70:45–52
16. Chen JX, Lin SW, Bing WH (2014) Geometric error measurement and identification for rotary table of multi-axis machine tool using double ball bar. Int J Mach Tools Manuf 77:47–55
17. Liu SJ, Watanabe K, Chen X (2009) Profile measurement of a wide-area resist surface using a multi-ball cantilever system. Precis Eng 33:50–55
18. Veeco (2006) Instruments Forms Process Equipment Group. III-VS Review
19. Adamczak S, Orzechowski T, Stanczyk TL (2007) The infrared measurement of form deviations of machine parts in motion. Measurement 40:28–35